Received: 4 July 2019 | Revised: 30 September 2019 | Accepted: 30 September 2019

DOI: 10.1002/jccs.201900268

JOURNAL OF THE CHINESE CHEMICAL SOCIETY

ARTICLE

Benzoylquinazolinone derivatives as new potential antidiabetic agents: α-Glucosidase inhibition, kinetic, and docking studies

Maryam Mohammadi-Khanaposhtani[1] | Hoda Yahyavi[2] | Somaye Imanparast[3] | Fereshte Nazemi Harandi[4] | Mohammad Ali Faramarzi[3] | Alireza Foroumadi[2] | Bagher Larijani[5] | Mahmood Biglar[5] | Mohammad Mahdavi[5]

[1]Cellular and Molecular Biology Research Center, Health Research Institute, Babol University of Medical Sciences, Babol, Iran

[2]Department of Medicinal Chemistry, Faculty of Pharmacy and Pharmaceutical Sciences Research Center, Tehran University of Medical Sciences, Tehran, Iran

[3]Department of Pharmaceutical Biotechnology, Faculty of Pharmacy and Biotechnology Research Center, Tehran University of Medical Sciences, Tehran, Iran

[4]Biotechnology Group, Chemical Engineering Department, Tarbiat Modares University, Tehran, Iran

[5]Endocrinology and Metabolism Research Center, Endocrinology and Metabolism Clinical Sciences Institute, Tehran University of Medical Sciences, Tehran, Iran

Correspondence
Bagher Larijanig and Mohammad Mahdavi, Endocrinology and Metabolism Research Center, Endocrinology and Metabolism Clinical Sciences Institute, Tehran University of Medical Sciences, Tehran, Iran.
Email: emrc@tums.ac.ir (B. L.) and momahdavi@tums.ac.ir (M. M.)

Abstract

Benzoylquinazolinone derivatives **3a–n** were synthesized via a simple one-step reaction, and evaluated for in vitro α-glucosidase inhibitory activity. Compounds **3d**, **3f–g**, **3i**, and **3m–n** showed more inhibitory activity than standard drug acarbose (IC_{50} = 750.0 ± 1.5 μM), and among them, compound **3d** displayed the highest α-glucosidase inhibitory activity (IC_{50} = 261.6 ± 0.1 μM). The kinetic analysis of the compound **3d** revealed that this compound inhibited α-glucosidase in a competitive manner (K_i = 255 μM). The docking studies were applied to predict binding modes of the synthesized compounds in active site of α-glucosidase.

KEYWORDS

antidiabetic, benzoylquinazolinone, kinetic analysis, α-glucosidase

1 | INTRODUCTION

The World Health Organization estimates that by 2030, more than 300 million people will be diagnosed with Type 2 diabetes.[1] Type 2 diabetes results from a combination of resistance to insulin action in body cell, impaired β-cell function, increased hepatic glucose production, and decreased insulin-mediated glucose uptake.[2] Current treatment modalities of this disease include exercise, diet, and various medical treatments. Available drugs for treatment of Type 2 diabetes act through delayed digestion and absorption of intestinal carbohydrates (α-glucosidase inhibitors), suppress hepatic glucose production (biguanides), stimulate insulin secretion (sulfonylureas and glinides), and improve insulin sensitivity and peripheral glucose uptake (thiazolidinediones and metformin). As mentioned, one way to reduce blood glucose in Type 2 diabetes is to decrease the absorption of glucose in intestine that is created by interfering with the action of α-glucosidases present in the small brush border. Acarbose and miglitol are α-glucosidase inhibitors that are today used to treat diabetes and are often associated with side

effects such as abdominal bloating, diarrhea, and flatulence.[3] On the other hand, there are some reports that show inhibition of the α-glucosidase can be valuable in the treatment of other carbohydrate-mediated illnesses such as cancer, viral infections, and hepatitis.[4–6] Thus, development of safe and effective inhibitors for α-glucosidase is an attractive subject for pharmaceutical chemists.[7–10]

Quinazolinone is an important scaffold with numerous pharmacological properties such as anticancer, anticonvulsant, anti-HIV, central nervous system depressant, anti-inflammatory, antifungal, antimicrobial activities.[11–17] Recently, new quinazolinone derivatives have been reported as potent α-glucosidase inhibitors.[18]

In our continued interest in the development of α-glucosidase inhibitors, we synthesized and evaluated benzoylquinazolinone derivatives **3a–n** as new inhibitors of α-glucosidase.[19–21] We also performed a molecular docking study to further investigate the interaction modes of these compounds in the active site of α-glucosidase.

2 | RESULTS AND DISCUSSION

2.1 | Chemistry

The target compounds **3a–n** were synthesized by a simple one-step reaction between acetophenones 1 and 2-aminobenzamide 2 in the presence of iodine in dimethyl sulfoxide (DMSO) at 100°C (Scheme 1) [22].

The target compounds **3a–n** were fully characterized by physical techniques. For example, nuclear magnetic resonance (NMR) spectra of the compound **3a** was assigned, as shown in Scheme 2.

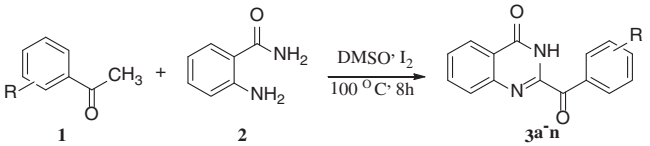

SCHEME 1 Synthetic protocol of quinolinone derivatives **3a–n**

2.2 | In vitro α-glucosidase inhibitory activity

α-Glucosidase inhibitory activity of benzoylquinazolinone derivatives **3a–n** was evaluated against α-glucosidase from *Saccharomyces cerevisiae* (yeast) and compared with acarbose as a standard drug. Table 1 shows the IC_{50} values of the synthesized compounds **3a–n**. Among these compounds, compounds **3d**, **3f–g**, **3i**, and **3m–n** displayed high inhibitory activities against α-glucosidase with the IC_{50} values in the range of 261.6 ± 0.1–494.1 ± 0.7 μM when compared with the standard drug acarbose. Compound **3d** was found to be the most potent inhibitor of α-glucosidase with the IC_{50} value of 261.6 ± 0.1 μM; compound **3h** was as potent as acarbose against α-glucosidase; and compounds **3a–c**, **3e**, and **3j–l** did not show any activity (Table 1).

Structure–activity relationship (SAR) analysis indicated that anti-α-glucosidase activity of this class of compounds depends mainly on the type and position of substituents on the aromatic side chain, derived from various acetophenones.

The results showed that the electronic properties of substituents on the aromatic side chain affect α-glucosidase inhibitory activity as no activity was observed for un-substituted compound **3a**. Compounds with electron-donating groups such as methyl, hydroxyl, and methoxy in any position of the phenyl group do not show anti-α-glucosidase activity as observed in compounds **3b–c**, **3j–l**. The presence of a halogen atom as electron-withdrawing substituent on the 4-position of phenyl group led to increased inhibitory activity and is demonstrated in compounds **3d** (IC_{50} = 261.6 ± 0.1 μM), **3f** (IC_{50} = 386.8 ± 0.9 μM), and **3i** (IC_{50} = 494.1 ± 0.7 μM) in the order of F > Cl > Br. On the other hand, 2-fluro and 2-chloro derivatives **3c** and **3e** do not show any α-glucosidase inhibitory activity. Moreover, the introduction of the second chlorine atom onto the 2-position of phenyl ring in compound **3f** (IC_{50} = 386.8 ± 0.9 μM) led to a decrease in inhibitory activity as observed in compound **3g** (IC_{50} = 406.5 ± 0.9 μM). 3-Bromo derivative **3h** (IC_{50} = 759.6 ± 0.7 μM) showed inhibitory activity similar to acarbose against α-glucosidase. Interestingly, the second and the third most potent compounds against α-glucosidase

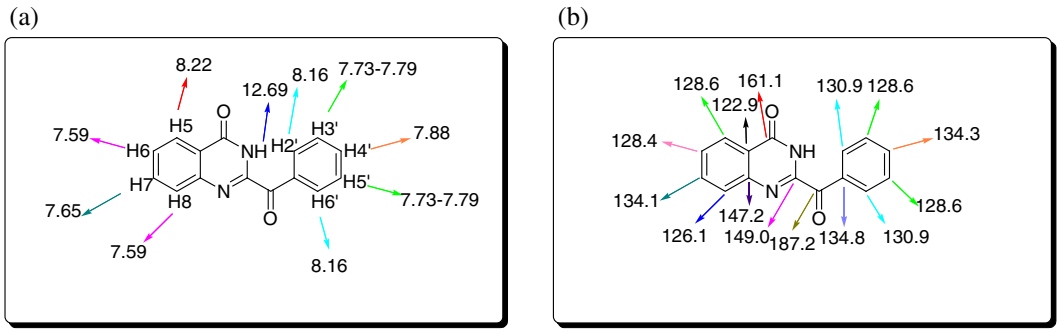

SCHEME 2 Selected ^{1}H NMR (a) and ^{1}H CNMR (b) data of the compound **3a** (unit of numbers in the scheme is ppm)

TABLE 1 In vitro α-glucosidase inhibitory activity of the synthesized compounds **3a–n**

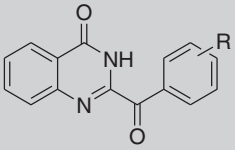

Compound	R	IC_{50} (μM)[a]	Compound	R	IC_{50} (μM)[a]
3a	H	NA	**3h**	3-Br	759.6 ± 0.7
3b	4-CH_3	NA	**3i**	4-Br	494.1 ± 0.7
3c	2-F	NA	**3j**	4-OH	NA
3d	4-F	261.6 ± 0.1	**3k**	3-OCH_3	NA
3e	2-Cl	NA	**3l**	4-OCH_3	NA
3f	4-Cl	386.8 ± 0.9	**3m**	2-NO_2	368.0 ± 0.9
3g	2,4-Dichloro	406.5 ± 0.9	**3n**	4-NO_2	296.7 ± 0.9
Acarbose	—	750.0 ± 1.5	Acarbose	—	750.0 ± 1.5

Abbreviation: NA, not active.

[a]Values are mean ± *SD*. All experiments were performed at least three times.

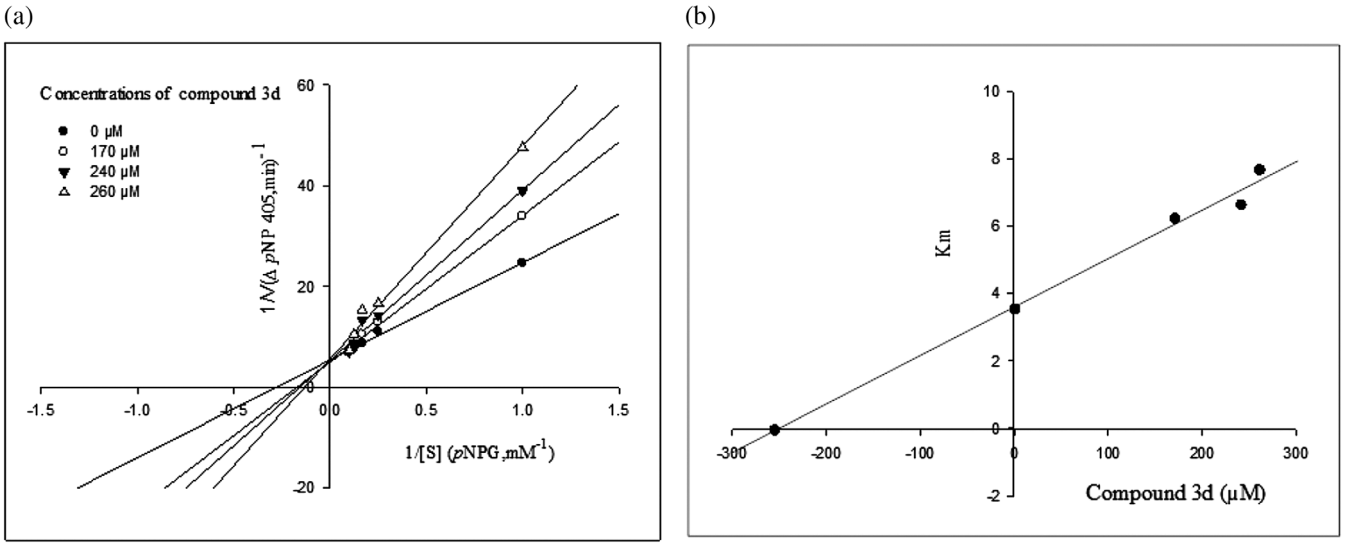

FIGURE 1 Kinetic of α-glucosidase inhibition by the compound **3d**. (a) The Lineweaver–Burk plot in the absence and presence of different concentrations of the compound **3d**. (b) The secondary plot between K_m and various concentrations of the compound **3d**

were derivatives **3n** (IC_{50} = 296.7 ± 0.9 μM) and **3m** (IC_{50} = 368.0 ± 0.9 μM) with strong electron-withdrawing group NO_2, respectively, in 4- and 2-position of pendant phenyl ring.

2.3 | Kinetic study

The kinetic study of the most potent compound **3d** against α-glucosidase was performed using a Lineweaver–Burk plot according to literature procedure (Figure 1a). Figure 1b shows secondary replot of 1/v versus 1/[S], for the enzyme, in the presence of compound **3d**. The Lineweaver–Burk plot showed that in the presence of compound **3d**, the values of V_{max} remained unchanged, while the values of K_m increased with increasing concentrations of the inhibitor. This indicates that compound **3d** acted as a competitive inhibitor of the α-glucosidase. The K_i (inhibitor constant) was calculated directly by secondary replot of Lineweaver–Burk plots. The K_i value of compound **3d** was 255 μM.

2.4 | Docking study

To study the interaction modes of the synthesized compounds in the active site of α-glucosidase and their related inhibitory activities, docking study was performed using Auto Dock Tools (version 1.5.6). Since we used *S. cerevisiae* α-glucosidase in the Section 3 and it did not have any crystallographic structure in the PDB, for docking purposes we applied the crystal structure of isomaltase (PDB code 3A4A) from *S. cerevisiae* with 71% identity and 84% similarity to *S. cerevisiae* α-glucosidase.[23]

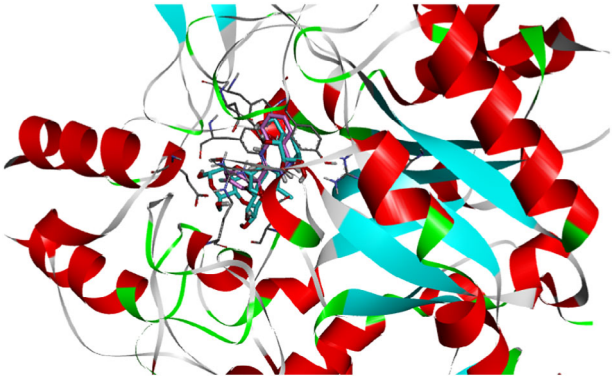

FIGURE 2 Superimposition of **3d** (pink) and acarbose (cyan) in the α-glucosidase active site

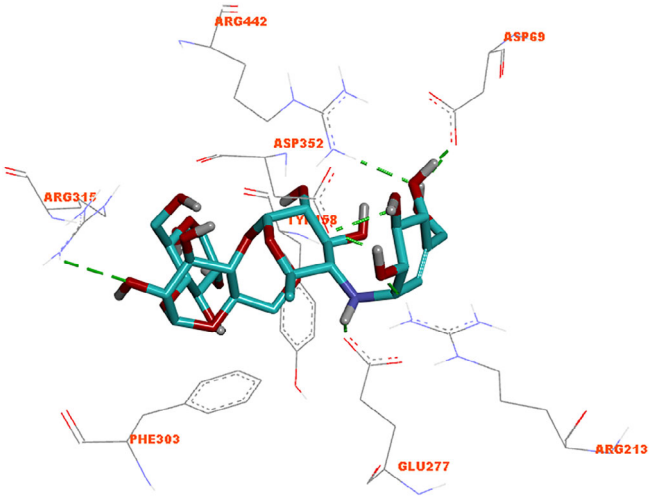

FIGURE 3 Binding mode of acarbose in the in the enzyme active site

Acarbose, the most potent compound **3d,** and inactive compound **3c** were docked in the active site of isomaltase. Figure 2 shows the superposed structure of acarbose as a standard inhibitor and the most potent compound **3d** in the active site of isomaltase.

The detailed binding mode of acarbose showed that this drug formed six hydrogen bond interactions with residues Asp69, Arg213, Glu277, Arg315, Asp352, and Arg442 in the enzyme active site (Figure 3).

The most active compound **3d** established hydrogen bonds with active site residues Arg213 and Asp352 through carbonyl and NH unit of quinazolinone moiety (Figure 4). In addition, this compound formed three π-π interactions with Tyr72, Phe178, and Tyr158 and three π-anion interactions with Asp69, Arg442, and Glu411. In addition, 4-fluoro substituent of pendant phenyl group interacted with Tyr158 (Figure 4). In the case of compound **3c**, the presence of a fluorine atom at the 2-position of pendant benzyl group leads to the loss of inhibitory activity. This finding can be reasonably explained by the interaction between 2-flouro substituent and carbonyl unit attached to quinazolinoe moiety (Figure 4). Although this compound interacts with important residues Arg213, Glu277, Arg315, Asp352, and Arg442 in the active site, it appears that internal interaction of 2-flouro substituent leads to inappropriate interactions of compound **3c** with the active site of enzyme.

3 | EXPERIMENTAL

3.1 | General

All chemicals were purchased from Merck (Germany) and were used without further purification. Melting points were measured on an Electro thermal 9100 apparatus and are uncorrected. IR spectra were recorded on a Shimadzu IR-460 spectrometer. ^{1}H and ^{13}C NMR spectra were measured (DMSO solution) with Bruker DRX-500 AVANCE (at 500.1 and 125.8 MHz) with TMS as an internal standard. Mass spectroscopy was performed on an Agilent Technology (HP) operating at an ionization potential of 70 eV. Elemental analysis was obtained with an Elementar Analysen system GmbH VarioEL (CHN mode).

3.2 | General procedure for the synthesis of synthesis of benzoylquinazolinone derivatives 3a–n

Acetophenones 1 (1 mmol) were added to a stirring solution of 2-aminobenzamide 2 (1 mmol) and iodine (1.2 mmol) in DMSO (3 ml) in a dropwise manner during 30 min. The reaction mixture was stirred at 100°C for 8 hr. After reaction completion, the reaction mixture was poured into cold water and excess iodine was neutralized with sodium thiosulfate. Then, the mixture was extracted using dichloromethane (2 × 25 ml) and the solvent was evaporated under reduced pressure. Finally, the residue was purified using recrystallization from ethyl acetate to obtain pure products **3a–n** (75–85%).

3.3 | Spectral data

3.3.1 | 2-benzoylquinazolin-4(3H)-one (3a)

White powder, yield: 84%, mp 184–186°C, IR (KBr) (ν_{max}/cm^{-1}): 3,175, 3,063, 3,232, 2,918, 1,704, 1,680, 1,593, 1,447, 1,305, 1,242, 893, 776, 689. ^{1}H NMR (500 MHz, DMSO-d_6): 7.59 (t, J = 7.5 Hz, 2H), 7.65 (t, J = 7.5 Hz, 1H), 7.73–7.79 (m, 2H), 7.88 (t, J = 7.5 Hz, 1H), 8.16 (t, J = 8 Hz, 2H), 8.22 (d, J = 8 Hz, 1H), 12.69 (s, NH). ^{13}C NMR (125 MHz, DMSO-d_6): δ 122.9 (C–CO), 126.1 (CH), 128.4 (CH), 128.6 (3CH), 130.9 (2CH), 134.1 (CH), 134.3 (C–CO), 134.8 (CH), 147.2 (C–N), 149.0 (N–C–N), 161.1 (C=O),

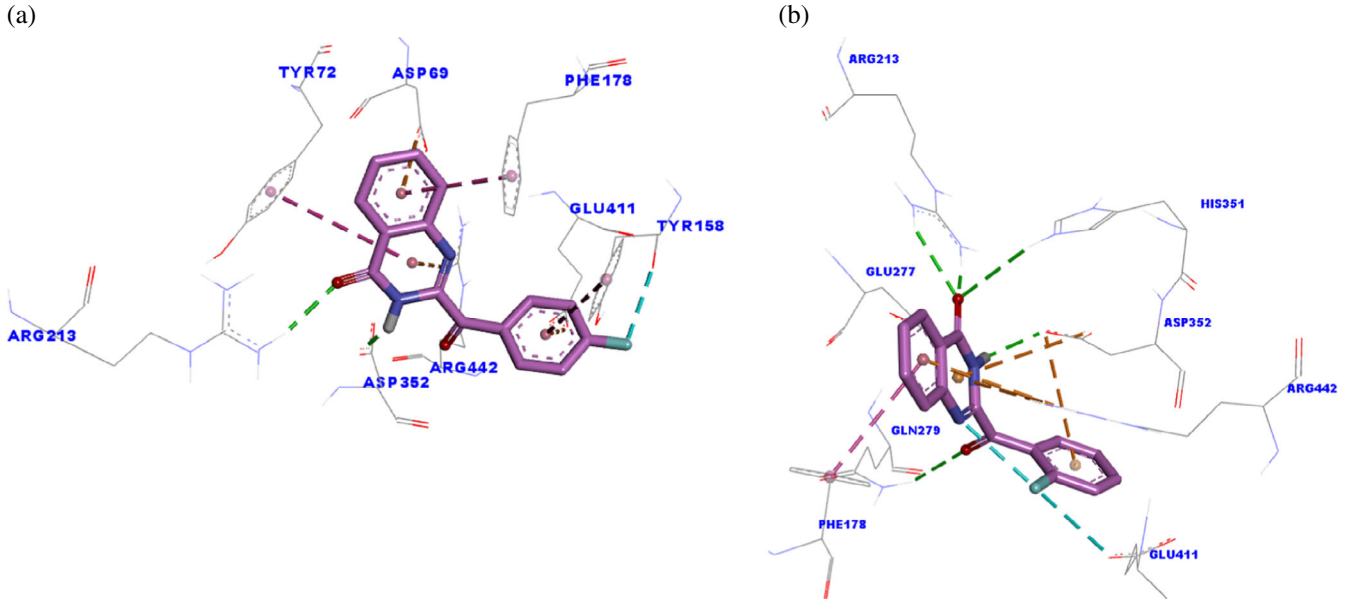

FIGURE 4 Docking poses of the compounds **3d** (a) and **3c** (b) in the active site of enzyme

187.2 (C=O). MS (70 eV): m/z = 250 (M+). $C_{15}H_{10}N_2O_2$ (250.25): calcd. C 71.99, H 4.03, N 11.19; found C 71.84, H 4.12, N 11.01.

3.3.2 | 2-(4-methylbenzoyl)quinazolin-4(3H)-one (3b)

White powder, yield: 82%, mp 225–229°C, IR (KBr) (ν_{max}/cm^{-1}): 3,171, 3,134, 3,090, 3,070, 2,918, 1,666, 1,601, 1,464, 1,436, 1,335, 1,288, 1,157, 1,099, 898, 769. ^{1}H NMR (500 MHz, DMSO-d_6): 2.42 (s, 3H), 7.11 (d, J = 9 Hz, 2H), 7.64 (t, J = 7.5 Hz, 1H), 7.77 (d, J = 8.5 Hz, 1H), 7.88 (t, J = 7.5 Hz, 1H), 8.19 (m, 3H), 12.68 (s, NH). ^{13}C NMR (125 MHz, DMSO-d_6): δ 55.8 (OCH_3), 114.1 (2CH), 122.7 (C–CO), 126.0 (CH), 126.4 (CH), 128.2 (CH), 128.4 (CH), 133.5 (2CH), 134.8 (C–CO), 147.2 (C–N), 149.6 (N–C–N), 161.1 (C=O), 164.3 (OCH_3), 186.7 (C=O). MS (70 eV): m/z = 264 (M+). $C_{16}H_{12}N_2O_2$ (264.28): calcd. C 72.72, H 4.58, N 10.60; found C 72.91, H 4.34, N 10.49.

3.3.3 | 2-(2-fluorobenzoyl)quinazolin-4(3H)-one (3c)

White powder, yield: 79%, mp 244–248°C, IR (KBr) (ν_{max}/cm^{-1}): 3,174, 3,035, 2,917, 1,697, 1,606, 1,488, 1,449, 1,313, 1,227, 1,176, 1,100, 899, 751. ^{1}H NMR (500 MHz, DMSO-d_6): 7.40 (m, 2H), 7.66 (t, J = 8 Hz, 4H), 7.71 (d, J = 8 Hz, 1H), 7.73–7.75 (m, 1H), 7.86 (t, J = 8 Hz, 1H), 7.90 (t, J = 7 Hz, 1H), 8.21 (d, J = 7.5 Hz, 1H), 12.81 (s, NH). ^{13}C NMR (125 MHz, DMSO-d_6): δ 116.5 (J = 85 Hz, CH), 122.9 (C–CO), 123.8 (J = 45 Hz, C–F), 124.7 (CH), 126.2 (CH), 128.4 (CH), 128.9 (CH), 132.0 (CH), 134.9 (C–CO), 135.6 (J = 33 Hz,CH), 147.1 (C–N), 148.9 (N–C–N), 160.8 (J = 1,010 Hz, C–F), 161.0 (C=O), 186.1 (C=O). $C_{15}H_9FN_2O_2$ (268.24): calcd. C 67.16, H 3.38, N 10.44; found C 67.24, H 3.55, N 10.31.

3.3.4 | 2-(4-Fluorobenzoyl)quinazolin-4(3H)-one (3d)

Yellow powder, yield: 81%, mp 232–235°C, IR (KBr) (ν_{max}/cm^{-1}): 3,187, 3,072, 2,921, 1,681, 1,596, 1,506, 1,447, 1,438, 1,336, 1,230, 1,158, 1,100, 900, 843, 771. ^{1}H NMR (500 MHz, DMSO-d_6): 7.42 (t, J = 8.5 Hz, 2H), 7.65 (t, J = 7 Hz, 1H), 7.78 (d, J = 8 Hz, 2H), 7.88 (t, J = 7.5 Hz, 1H), 8.21 (d, J = 7.5 Hz, 1H), 8.28 (t, J = 7 Hz, 2H), 12.68 (s, NH). ^{13}C NMR (125 MHz, DMSO-d_6): δ 115.8 (2CH, J = 87.5 Hz), 122.8 (C–CO), 126.1 (CH), 128.5 (2CH, J = 124.5 Hz), 130.8 (CH), 134.1 (CH, J = 37.5 Hz), 134.7 (C–CO), 147.1 (C–N), 149.0 (N–C–N), 161.3 (C=O), 165.6 (C–F, J = 1,010 Hz), 185.7 (C=O). $C_{15}H_9FN_2O_2$ (268.24): calcd. C 67.16, H 3.38, N 10.44; found C 66.95, H 3.51, N 10.32.

3.3.5 | 2-(2-chlorobenzoyl)quinazolin-4(3H)-one (3e)

Yellow powder, yield: 76%, mp 245–247°C, IR (KBr) (ν_{max}/cm^{-1}): 3,172, 2,915, 1,709, 1,608, 1,529, 1,447, 1,343, 1,239, 1,128, 869, 769. ^{1}H NMR (500 MHz, DMSO-d_6): 7.51 (t, J = 7.5 Hz, 1H), 7.60–7.69 (m, 4H), 7.79 (d, J = 7.5 Hz, 1H), 7.84 (t, J = 8 Hz, 1H), 8.21 (d, J = 7.5 Hz, 1H), 12.78 (s, NH). ^{13}C NMR (125 MHz, DMSO-d_6): δ 123.0 (C–CO), 126.2 (CH), 127.2 (CH), 128.6 (C), 129.2

(CH), 130.0 (CH), 131.3 (2CH), 133.2 (CH), 134.9 (C–CO), 135.5 (CH), 147.1 (C–N), 148.3 (N–C–N), 161.1 (C=O), 188.8 (C=O). $C_{15}H_9ClN_2O_2$ (284.70): calcd. C 63.28, H 3.19, N 9.84; found C 63.41, H 3.35, N 10.07.

3.3.6 | 2-(4-chlorobenzoyl)quinazolin-4(3H)-one (3f)

White powder, yield: 83%, mp 238–240°C, IR (KBr) (ν_{max}/cm^{-1}): 3,173, 3,095, 1,662, 1,586, 1,465, 1,336, 1,286, 1,148, 1,091, 898, 848, 772. ^{1}H NMR (500 MHz, DMSO-d_6): 7.60–7.66 (m, 3H), 7.91 (t, J = 7.5 Hz, 1H), 8.30 (t, J = 8 Hz, 2H), 8.43 (d, J = 8 Hz, 1H), 11.25 (s, NH). $C_{15}H_9ClN_2O_2$ (284.70): calcd. C 63.28, H 3.19, N 9.84; found C 63.06, H 3.26, N 10.11.

3.3.7 | 2-(2,5-dichlorobenzoyl)quinazolin-4(3H)-one (3g)

White powder, yield: 84%, mp 243–245°C, IR (KBr) (ν_{max}/cm^{-1}): 3,175, 3,093, 1,661, 1,588, 1,467, 1,335, 1,287, 1,148, 1,090, 896, 848, 771. ^{1}H NMR (500 MHz, DMSO-d_6): 7.62–7.70 (m, 3H), 7.82–7.86 (m, 3H), 8.21 (d, J = 7.5 Hz, 1H), 12.90 (s, NH). ^{13}C NMR (125 MHz, DMSO-d_6): δ 123.1 (C–CO), 126.2 (CH), 127.4 (CH), 128.6 (C), 129.3 (CH), 129.5 (CH), 132.4 (CH), 132.7 (C), 134.3 (CH), 134.8 (C–CO), 136.9 (CH), 146.9 (C–N), 147.9 (N–C–N), 161.0 (C=O), 187.7 (C=O). $C_{15}H_8Cl_2N_2O_2$ (319.14): calcd. C 56.45, H 2.53, N 8.78; found C 56.57, H 2.74, N 8.59.

3.3.8 | 2-(3-bromobenzoyl)quinazolin-4(3H)-one (3h)

White powder, yield: 77%, mp 220–223°C, IR (KBr) (ν_{max}/cm^{-1}): 3,175, 3,091, 1,660, 1,582, 1,464, 1,438, 1,336, 1,283, 1,146, 1,010, 896, 771. ^{1}H NMR (500 MHz, DMSO-d_6): 7.55 (t, J = 7.5 Hz, 1H), 7.66 (t, J = 7.5 Hz, 1H), 7.79 (d, J = 8 Hz, 1H), 7.89 (t, J = 7.5 Hz, 1H), 7.94 (d, J = 8 Hz, 1H), 8.16 (d, J = 7.5 Hz, 1H), 8.22 (d, J = 8.5 Hz, 1H), 8.34 (s, 1H), 12.68 (s, NH). ^{13}C NMR (125 MHz, DMSO-d_6): δ 121.5 (C–Br), 123.0 (C–CO), 126.0 (CH), 128.4 (CH), 128.8 (CH), 129.8 (CH), 130.7 (CH), 133.3 (CH), 134.8 (C–CO), 136.2 (CH), 136.5 (CH), 148.4 (C–N), 149.9 (N–C–N), 161.1 (C=O), 185.8 (C=O). $C_{15}H_9BrN_2O_2$ (329.15): calcd. C 54.74, H 2.76, N 8.51; found C 54.59, H 2.65, N 8.38.

3.3.9 | 2-(4-bromobenzoyl)quinazolin-4(3H)-one (3i)

White powder, yield: 79%, mp 275–277°C, IR (KBr) (ν_{max}/cm^{-1}): 3,176, 3,091, 1,662, 1,580, 1,465, 1,438, 1,336, 1,284, 1,147, 1,011, 897, 770. ^{1}H NMR (500 MHz, DMSO-d_6): 7.59 (t, J = 7.5 Hz, 2H), 7.65 (t, J = 7.5 Hz, 1H), 7.73–7.79 (m, 2H), 7.88 (t, J = 7.5 Hz, 1H), 8.16 (t, J = 8 Hz, 2H), 8.22 (d, J = 8 Hz, 1H), 12.69 (s, NH). ^{13}C NMR (125 MHz, DMSO-d_6): δ 122.8 (C–CO), 125.9 (CH), 126.0 (CH), 128.4 (CH), 131.5 (2CH), 132.6 (CH), 132.8 (2CH), 133.1 (CH), 134.7 (C–CO), 146.9 (C–N), 148.4 (N–C–N), 160.9 (C=O), 186.0 (C=O). MS (70 eV): m/z = 329 (M+). $C_{15}H_9BrN_2O_2$ (329.15): calcd. C 54.74, H 2.76, N 8.51; found C 54.86, H 2.68, N 8.34.

3.3.10 | 2-(4-hydroxybenzoyl)quinazolin-4(3H)-one (3j)

Yellow powder, yield: 75%, mp 226–230°C, IR (KBr) (ν_{max}/cm^{-1}): 3,247, 1,683, 1,650, 1,604, 1,512, 1,462, 1,440, 1,300, 1,225, 1,163, 902, 768. ^{1}H NMR (500 MHz, DMSO-d_6): 6.93 (d, J = 8.5 Hz, 2H), 7.62 (t, J = 7 Hz, 1H), 7.77 (d, J = 8 Hz, 1H), 7.86 (t, J = 7 Hz, 1H), 8.09 (d, J = 7 Hz, 2H), 8.20 (d, J = 8 Hz, 1H), 12.61 (s, NH). ^{13}C NMR (125 MHz, DMSO-d_6): δ 115.5 (2CH), 122.6 (C–CO), 125.2 (CH), 126.0 (CH), 128.2 (CH), 133.5 (CH), 133.8 (2CH), 134.7 (C–CO), 147.3 (C–N), 149.9 (N–C–N), 161.1 (C=O), 163.6 (C–OH), 185.1 (C=O). $C_{15}H_{10}N_2O_3$ (266.25): calcd. C 67.67, H 3.79, N 10.52; found C 67.48, H 3.85, N 10.73.

3.3.11 | 2-(3-methoxybenzoyl)quinazolin-4(3H)-one (3k)

Yellow powder, yield: 83%, mp 186–190°C, IR (KBr) (ν_{max}/cm^{-1}): 3,070, 2,965, 1,699, 1,674, 1,595, 1,486, 1,445, 1,332, 1,230, 1,158, 1,100, 900, 843, 771. ^{1}H NMR (500 MHz, DMSO-d_6): 3.82 (s, OCH_3), 7.30 (d, J = 7.5 Hz, 1H), 7.49 (t, J = 8 Hz, 1H), 7.63 (t, J = 7 Hz, 1H), 7.70(s, 1H), 7.74 (d, J = 7.5 Hz, 1H), 7.78 (d, J = 7.5 Hz, 1H), 7.86 (t, J = 7.5 Hz, 1H), 8.21 (d, J = 8 Hz, 1H), 12.67 (s, NH). ^{13}C NMR (125 MHz, DMSO-d_6): δ 55.4 (OCH_3), 114.9 (CH), 120.3 (CH), 122.9 (C–CO), 123.6 (CH), 126.0 (CH), 128.3 (CH), 128.6 (CH), 129.7 (CH), 134.8 (C–CO), 135.3 (CH), 147.1 (C–N), 149.0 (N–C–N), 159.1 (C–OCH_3), 161.1 (C=O), 186.7 (C=O). $C_{16}H_{12}N_2O_3$ (280.28): calcd. C 68.56, H 4.32, N 9.99; found C 68.41, H 4.19, N 10.13.

3.3.12 | 2-(4-methoxybenzoyl)quinazolin-4(3H)-one (3l)

Yellow powder, yield: 85%, mp 186–190°C, IR (KBr) (ν_{max}/cm^{-1}): 3,170, 3,061, 2,963, 2,840, 1,677, 1,601, 1,505, 1,445, 1,339, 1,241, 1,162, 1,028, 897, 778. ^{1}H NMR (500 MHz, DMSO-d_6): 3.88 (s, 3H, OCH_3), 7.11 (d, J = 8 Hz, 2H), 7.64 (t, J = 7.5 Hz, 1H), 7.77 (d, J = 8 Hz, 2H), 7.87 (t, J = 7.5 Hz, 1H), 8.07 (d, J = 8 Hz, 2H), 8.21 (d, J = 7.5 Hz,

1H), 12.62 (s, NH). ^{13}C NMR (125 MHz, DMSO-d_6): δ 21.4 (CH_3), 122.8 (C–CO), 126.1 (CH), 128.3 (CH), 128.5 (CH), 129.2 (2CH), 131.0 (2CH), 131.5 (CH), 134.8 (C–CO), 145.2 (C–CH_3), 147.2 (C–N), 149.3 (N–C–N), 161.1 (C=O), 186.7 (C=O).). $C_{16}H_{12}N_2O_3$ (280.28): calcd. C 68.56, H 4.32, N 9.99; found C 68.32, H 4.03, N 9.78.

3.3.13 | 2-(2-nitrobenzoyl)quinazolin-4(3H)-one (3m)

Yellow powder, yield: 75%, mp 300°C, IR (KBr) (ν_{max}/cm^{-1}): 3,172, 2,915, 1,709, 1,608, 1,529, 1,447, 1,343, 1,239, 1,128, 869, 769. ^{1}H NMR (500 MHz, DMSO-d_6): 7.51(d, J = 7 Hz, 2H), 7.63 (t, J = 7.5 Hz, 1H), 7.80–7.95 (m, 3H), 7.99 (t, J = 7.5 Hz, 1H), 8.18 (d, J = 7 Hz, 1H), 8.27 (d, J = 7.5 Hz, 2H), 13.00 (s, NH). ^{13}C NMR (125 MHz, DMSO-d_6): δ 123.0 (C–CO), 123.9 (CH), 126.3 (CH), 128.4 (CH), 129.3 (CH), 130.4 (CH), 132.3 (CH), 132.5 (CH), 135.0 (C–CO), 135.1 (CH), 146.7 (C–NO_2), 147.5 (C–N), 147.9 (N–C–N), 160.0 (C=O), 187.2 (C=O). MS (70 eV): m/z = 295 (M+). $C_{15}H_9N_3O_4$ (295.25): calcd. C 61.02, H 3.07, N 14.23; found C 60.89, H 3.21, N 14.07.

3.3.14 | 2-(3-nitrobenzoyl)quinazolin-4(3H)-one (3n)

Yellow powder, yield: 78%, mp 272–275°C, IR (KBr) (ν_{max}/cm^{-1}): 3,048, 2,923, 1,708, 1,681, 1,607, 1,530, 1,447, 1,352, 1,242, 1,129, 1,096, 918, 771. ^{1}H NMR (500 MHz, DMSO-d_6): 7.67 (t, J = 7.5 Hz, 2H), 7.78 (d, J = 7.5 Hz, 1H), 7.85–7.90 (m, 2H), 7.88 (t, J = 7.5 Hz, 1H), 8.22 (d, J = 7.5 Hz, 1H), 8.53 (d, J = 7.5 Hz, 1H), 8.58 (d, J = 7.5 Hz, 1H), 8.99 (s, 1H), 12.77 (s, NH). ^{13}C NMR (125 MHz, DMSO-d_6): δ 122.1 (C–CO), 125.7 (CH), 125.8 (CH), 126.1 (CH), 128.5 (CH), 129.0 (CH), 130.1 (CH), 134.8 (CH), 135.6 (CH), 137.0 (C–CO), 146.9 (C–N), 147.4 (C–NO_2), 148. 1 (N–C–N), 161.2 (C=O), 185.1 (C=O). MS (70 eV): m/z = 295 (M+). $C_{15}H_9N_3O_4$ (295.25): calcd. C 61.02, H 3.07, N 14.23; found C 61.24, H 2.91, N 14.44.

3.4 | α-Glucosidase inhibition assay

Determination of α-glucosidase inhibitory activity of synthesized compounds **3a–n** was performed exactly based on our previous report [21].

3.5 | Kinetic study

Kinetic study was carried out to determine the inhibition mode of the title compounds. Twenty microliters of enzyme solution (1 U/ml) was incubated with concentrations 0, 170, 240, and 260 μM of the most potent compound **3d** for 15 min at 30°C. The reaction was then initiated by adding different concentrations of p-nitrophenyl glucopyranoside (1–4 mM) as substrate, and change in absorbance was determined for 20 min at 405 nm by using the spectrophotometer (Gen5, Power wave xs2, BioTek, America).

3.6 | Docking study

Docking studies were performed using Auto Dock Tools (version 1.5.6) on the pdb structure of 3A4A that was taken from the Brookhaven protein database (http://www.rcsb.org). The 3D structures of the selected compounds **3c** and **3d** were created by MarvineSketch 5.8.3, 2012, ChemAxon (http://www.chemaxon.com) and converted to pdbqt form using Auto Dock Tools. Also, the pdbqt form of protein was procured using the same software. Before preparation of Auto Dock format of enzyme, the additional molecules (water molecules and the inhibitors) were removed from it. Then, polar hydrogen atoms were added, Koullman charges were assigned, and the obtained protein was used as an input file for the AUTOGRID program. In AUTOGRID for each atom type in the ligand, maps were determined with 0.375 Å spacing between grid points, and the coordinates x, y, and z for the center of grid box were 22.625, −8.069, 24.158, respectively. The dimensions of the grid box were set at 50 × 50 × 50 Å. Flexible ligand dockings were accomplished for the selected inhibitors. For each docked system 50 runs of the AUTODOCK search by the Lamarckian genetic algorithm was carried. The best pose of each ligand was selected for analyzing the interactions between α-glycosidase and the ligand and visualized using Discovery Studio 4.0 Client.

4 | CONCLUSIONS

In conclusion, a series of benzoylquinazolinone derivatives **3a–n** was introduced as α-glucosidase inhibitor. 4-fluoro derivative **3d** was the most active compound, being around three times more potent than reference drug acarbose. Kinetic study of compound **3d** revealed that this compound inhibited α-glucosidase in a competitive manner. Furthermore, a docking study showed that the most active compound **3d** interacted properly with important amino acids in the active site of the enzyme. Due to the significant inhibitory activity of the compound **3d** against α-glucosidase, in vivo evaluation of this compound on streptozotocin-diabetic rats will be done in the future.

ORCID

Mohammad Mahdavi https://orcid.org/0000-0003-0256-3352

REFERENCES

[1] K. Ogurtsova, J. D. da Rocha Fernandes, Y. Huang, U. Linnenkamp, L. Guariguata, N. H. Cho, D. Cavan, J. E. Shaw, L. E. Makaroff, *Diabetes Res. Clin. Pract.* **2017**, *128*, 40.

[2] S. H. Havale, M. Pal, *Bioorg. Med. Chem.* **2009**, *17*, 1783.

[3] R. Coniff, A. Krol, *Clin. Ther.* **1997**, *19*, 16.

[4] M. J. Humphries, K. Matsumoto, S. L. White, K. Olden, *Cancer Res.* **1986**, *46*, 5215.

[5] H. Park, K. Y. Hwang, K. H. Oh, Y. H. Kim, J. Y. Lee, K. Kim, *Bioorg. Med. Chem.* **2008**, *16*, 284.

[6] S. J. Storr, L. Royle, C. J. Chapman, U. M. A. Hamid, J. F. Robertson, A. Murray, R. A. Dwek, P. M. Rudd, *Glycobiology* **2008**, *18*, 456.

[7] O. U. R. Abid, M. Ayaz, W. Rehman, K. Mehdi, A. Ali, A. Wadood, F. Rahim, A. Sultan, M. Ghufran, S. Mir, M. T. Qureshi, *J. Chin. Chem. Soc.* **2016**, *63*, 1015.

[8] S. Hameed, F. Seraj, R. Rafique, S. Chigurupati, A. Wadood, A. U. Rehman, V. Venugopal, U. Salar, M. Taha, K. M. Khan, *Eur. J. Med.Chem.* **2019**, *183*, 111677.

[9] M. Taha, S. Sultan, S. Imran, F. Rahim, K. Zaman, A. Wadood, A. U. Rehman, N. Uddin, K. M. Khan, *Bioorg. Med. Chem.* **2019**, *27*, 4081.

[10] G. Lavanya, K. Venkatapathy, C. J. Magesh, M. Ramanathan, R. Jayasudha, *Bioorg. Chem.* **2019**, *84*, 125.

[11] K. M. Chang, L. C. Chen, C. C. Tzeng, Y. H. Lu, I. L. Chen, S. H. Juang, T. C. Wang, *J. Chin. Chem. Soc.* **2018**, *65*, 1110.

[12] H. Georgey, N. Abdel-Gawad, S. Abbas, *Molecules* **2008**, *13*, 2557.

[13] C. E. Brown, T. Kong, J. McNulty, L. D'Aiuto, K. Williamson, L. McClain, P. Piazza, V. L. Nimgaonkar, *Bioorg. Med. Chem. Lett.* **2017**, *27*, 4601.

[14] S. K. Kashaw, V. Kashaw, P. Mishra, N. K. Jain, *Arkivoc* **2008**, *14*, 17.

[15] V. Alagarsamy, V. Raja Solomon, R. V. Sheorey, R. Jayakumar, *Chem. Biol. Drug. Des.* **2009**, *73*, 471.

[16] J. Zhang, J. Liu, Y. Ma, D. Ren, P. Cheng, J. Zhao, F. Zhang, Y. Yao, *Bioorg. Med. Chem. Lett.* **2016**, *26*, 2273.

[17] P. M. Bedi, V. Kumar, M. P. Mahajan, *Bioorg. Med. Chem. Lett.* **2004**, *14*, 5211.

[18] M. Wei, W. M. Chai, R. Wang, Q. Yang, Z. Deng, Y. Peng, *Bioorg. Med. Chem. Lett.* **2017**, *25*, 1303.

[19] M. Mohammadi-Khanaposhtani, H. Yahyavi, E. Barzegaric, S. Imanparast, M. M. Heravi, M. A. Faramarzi, A. Foroumadi, H. Adibi, B. Larijani, M. Mahdavi, *Polycycl. Aromat. Comp.* **2018**, 1. (in press)

[20] M. Mohammadi-Khanaposhtani, S. Rezaei, R. Khalifeh, S. Imanparast, M. A. Faramarzi, S. Bahadorikhalili, M. Safavi, F. Bandarian, E. N. Esfahani, M. Mahdavi, B. Larijani, *Bioorg. Chem.* **2018**, *80*, 288.

[21] M. Adib, F. Peytam, M. Rahmanian-Jazi, M. Mohammadi-Khanaposhtani, S. Mahernia, H. R. Bijanzadeh, M. Jahani, S. Imanparast, M. A. Faramarzi, M. Mahdavi, B. Larijani, *New J. Chem.* **2018**, *42*, 17268.

[22] Y. P. Zhu, Z. Fei, M. C. Liu, F. C. Jia, A. X. Wu, *Org. Lett.* **2012**, *15*, 378.

[23] H. Sun, W. Ding, X. Song, D. Wang, M. Chen, K. Wang, Y. Zhang, P. Yuan, Y. Ma, R. Wang, R. H. Dodd, *Bioorg. Med. Chem. Lett.* **2017**, *27*, 3226.

SUPPORTING INFORMATION

Additional supporting information may be found online in the Supporting Information section at the end of this article.

How to cite this article: Mohammadi-Khanaposhtani M, Yahyavi H, Imanparast S, et al. Benzoylquinazolinone derivatives as new potential antidiabetic agents: α-Glucosidase inhibition, kinetic, and docking studies. *J Chin Chem Soc*. 2019;1–8. https://doi.org/10.1002/jccs.201900268